

Response coefficient analysis of *E. coli* chemotaxis to parametric perturbations under the influence of noise

Pratap R. Patnaik

Received: 12 March 2013 / Received in revised form: 04 April 2013, Accepted: 04 June 2013 Published online: 30 June 2013
© Sevas Educational Society 2008-2013

Abstract

Escherichia coli and other bacteria navigating through ‘open’ environments are under the impact of noise from the environment and from within the cells. This generates fluctuations in the kinetic parameters that characterize the intra-cellular reactions of the chemosensory network, thus affecting the chemotaxis of the cells. This aspect has been studied here for *E. coli* synthesizing recombinant glucoamylase in a continuous-flow microreactor. Response coefficient analysis (RCA) was applied to a new four-parameter model of the chemotaxis of *E. coli*. The model considered two types of responses of the cells – linear and adaptive – and two rates of movement of the chemoattractant – slow and fast. Some cells at each position in the microreactor were considered to be moving to the left, some to the right and others in a tumbling state. Striking similarities and differences were observed between the different types of cells, between linear and adaptive responses, and between the kinetic responses to a slow-moving and a fast-moving chemoattractant distribution. One salient observation was that the response coefficients of the left-moving and right-moving sub-populations were mirror images of each other. Tumbling cells either had intermediate characteristics in some situations, as might be expected, or, in other circumstances, resembled the left-moving cells more than they corresponded to the right-moving bacteria. Under certain conditions, cells with normal linear responses exhibited pseudo-adaptive kinetic behavior. Such unexpected observations have been explained. The results offer new insights into possible quantitative effects of environmental noise on the chemotaxis of *E. coli* and other bacteria.

Keywords: *Escherichia coli*; Chemotaxis; Recombinant glucoamylase; Kinetic fluctuations; Performance variations; Response coefficient analysis.

Pratap R. Patnaik

Chemical Engineering Department, C. V. Raman College of Engineering, Bidyanagar, Mahura, Janla, Bhubaneswar-752054, India

* Tel: 00919040930337 Fax: 00916742113593;
Email: pratap.r.patnaik@gmail.com

Introduction

The movement of bacterial cells in response to chemical signals that are sensed has useful implications in a number of important areas such as wound healing (Agyingi et al. 2010), the operations of microfluidic systems for biochemical reactions (Ahmed et al. 2010) and the degradation of harmful chemicals in the environment (Pandey and Jain 2002, Singh and Olson 2008). Applications such as these, and the need to understand the chemosensory system from an evolutionary perspective as well as to design suitable genetically modified cells that are effective for specific requirements, have motivated many studies of bacterial chemotaxis.

Since the large number of studies of the chemotaxis of bacterial cells are discussed in detail in many recent reviews (Baker et al. 2006, Clauszitzner et al. 2010, Steuer et al. 2011, Tindall et al. 2008a, b), the mechanisms of chemotaxis will not be discussed here, except to present a brief overview of those features that are relevant to the present study. Many investigations have used *Escherichia coli* as a model system because it has a simple chemosensory network that contains all the important features of chemotaxis observed in other bacteria also (Hamadeh et al. 2011, Rao et al. 2004, Tindall et al. 2012). Moreover, the chemosensory network of *E. coli* has the smallest sufficiently robust network structure (Kollmann et al. 2005). Robustness has in fact been recognized as a distinctive feature of the chemotaxis of many bacteria that allows them to return to their pre-disturbed state on prolonged exposure to a disturbance. This is also the central theme of the work reported here because we show that robustness may not be sustained in all features if the disturbance(s) affects certain critical parameters of the chemosensory network.

The possibility of exposure to long-duration disturbances is realistic because the environmental conditions in which many bacteria function are not static or changing smoothly but contain fluctuations whose characteristics may vary with time (Patnaik 2006, Xu and Tao 2006). These fluctuations are often referred to as ‘noise’. In addition to noise from the environment, there are fluctuations inside the cells themselves, mainly due to the small sizes and concentrations of the biological molecules and variations in temperature, thus making reactions among them stochastic rather than deterministic (Kaern et al. 2005, Paulsson 2004, Raser and O’Shea 2005). In the case of bacterial chemotaxis, yet another source of noise that is partly associated with the cells is that present at the sites of chemical binding between the molecules in the

environment that initiate chemotaxis and the receptors of the cells that detect these molecule, bind to them and thereby generate a train of signals that eventually results in preferred movement of the cells toward the chemoattractant (Andrews et al. 2006, Hornung and Barkai 2008).

An important consequence of the noise-affected probabilistic collisions among the species involved in the chain of reactions that constitute the chemotactic signal propagation pathway is that the parameters of the component reactions are not 'crisp' well-defined constant numbers but may fluctuate with time. Since kinetic parameters depend on temperature, both molecular fluctuations and temperature fluctuations (Oleksink et al. 2011) contribute to variations in these parameters. The mechanistic basis and modeling of molecular kinetics under such conditions are elegantly discussed by Paulsson (2005), who pointed out that the noise present in cellular processes causes the 'parameters for protein synthesis (to) vary randomly' and to change dynamically as time progresses. This thesis is supported by his later work (Paulsson and Elf 2006), where quantitative effects on reaction rate equations are discussed.

Analyses such as these underline the significance of parametric fluctuations in determining the course of chemosensory signal transductions in a population of cells, and consequently the chemotaxis of the cells. As earlier studies have shown (Jiang et al. 2010, Patnaik 2008, Yi et al. 2000), response coefficient analysis provides a convenient and informative method to analyze the effects of small but sustained changes in reaction parameters on chemotactic performance. The present study therefore employs this method with an evolutionary model of chemotaxis proposed recently to evaluate the effects of parametric perturbations on population behavior.

Overview of *E. coli* Chemotaxis

Since a number of excellent tutorial articles have been published on the *E. coli* chemosensory system and its functioning (Baker et al. 2006, Berg 2000, Kollmann et al. 2005), only a short overview is provided here for readers not familiar with the subject.

The chemotactic movements of cells of *E. coli* are controlled by the chemosensory system shown schematically in Figure 1. The chemotaxis machinery is composed of broadly three main units: (i) chemoreceptors, which detect chemicals in the environment that are favorable to the cells and bind to them, (ii) a signal transduction

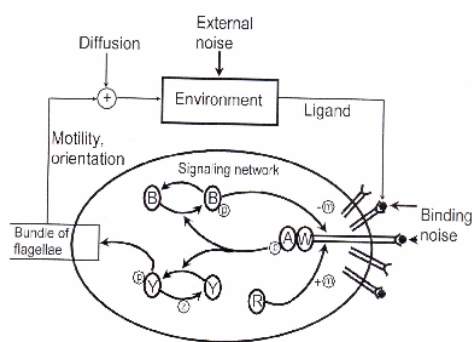


Figure 1. Pictorial representation of the chemosensory network of *Escherichia coli*. Modified and redrawn with permission from Andrews et al. (2006).

system that processes information received from the chemoreceptors, and generate instructions for (iii) the rotary motors,

which in turn rotate clockwise (CW) or counter-clockwise (CCW), thereby causing the cells to 'run' or 'tumble'. The last two terms are the final manifestations of chemotaxis, and they will be defined presently.

The response of the system is encoded by six essential genes – CheA, CheB, CheR, CheW, CheY and CheZ – and five partially redundant chemoreceptor genes – *aer*, *tap*, *tar*, *trg* and *tsr*. The epithet Che here signifies chemotaxis. CheA is a histidine protein-kinase that catalyzes the transfer of phosphoryl groups from ATP to one of its histidine imidazole side-chains, from where it is transferred to an aspartyl side-chain of the CheY protein. The phosphorylated CheY (CheY~P) then dissociates from CheA, diffuses through the cytoplasm and binds to the flagellar motor switch. The bound CheY~P functions as an allosteric regulator that governs the equilibrium between CW and CCW rotations of the motor. Fluorescence resonance energy transfer measurements indicate that non-phosphorylated CheY does not bind to the motors (Sourjik and Berg 2002). The phosphatase CheZ plays a key role in mediating the dephosphorylation of CheY~P (Vaknin et al. 2004).

The concentration of CheY~P is modulated through the five chemoreceptors – Aer, Tap, Tar, Trg and Tsr – each corresponding to one of the redundant chemoreceptor genes mentioned earlier. These receptors are structured as multimeric complexes that consist of dimers packed hexagonally into trimers (Briegleb et al. 2012, Francis et al. 2004) linked by the CheA and CheW proteins. As seen in Figure 1, the domains of the chemoreceptors that bind to compatible ligands of the chemoattractant molecules are outside the cytoplasmic membrane whereas the rest of the chemosensory network is in the cytosol. Binding of the receptors to the chemoattractant molecules triggers a sequence of events that culminates in CW or CCW rotation of the motors, thereby determining whether a cell will run or tumble until the next signal is received. A cardinal event in this sequence is reverse methylation of the receptor. Methylation has a complex role that is discussed elsewhere (Baker et al. 2006, Kollman et al. 2005, Rao et al. 2004), but one significant effect it has, apart from governing cell motility, is enhancement of robust perfect adaptation.

Briefly, robust perfect adaptation means that a population of cells exposed to a continuous disturbance (or noise) eventually reverts to its state before the start of the disturbance. Many, but not all, strains of *E. coli* possess this property. In other words, adaptation is widespread but not universal. Further, not all properties of a chemosensory network display robust perfect adaptation. The important of this caveat will be discussed later in the context of the results of the present work.

As stated above, the final effect of the propagation of a chemoattractant signal through a chemosensory network is the rotation of the flagella motors. This means the movements of a cell are executed through filamentous flagella that project outward and rotate either CW or CCW, depending on the direction of rotation of the motors that are attached to their bases. CCW rotation causes the flagella to move in a coordinated bundle, and the result is a straight line motion (called a 'run'). Likewise, CW rotation disentangles the flagella, causing the filaments to move independently and not in unison; the result is a change of orientation of the cell (i.e. a 'tumble'). For *E. coli* the duration of a run is typically about 1 sec, whereas a tumble takes about a tenth of this duration (Berg 2000). The main purpose of the tumbles is to reorient the cells frequently so that unidirectional runs do not lead a population away from the chemoattractant.

The durations of the runs and tumbles are short and comparable to the time scales of events in the chemosensory signal transduction pathway (Baker et al. 2006, Samuel and Berg 1995). Thus, it is realistically possible for fluctuations in cellular processes to interfere with the chemosensory response. While this postulate forms a basic tenet of the original Barkai-Leibler model (Alon et al. 1999), recent studies provide additional support to their hypothesis. One notable work is that of Korobkova and coworkers (2006), who showed that while stochastic fluctuations are possible, the time interval between the CW and CCW rotations of the flagellar motor of *E. coli* follows an exponential distribution. Nishikawa and Shibata's (2010) more recent work has shown that while bacteria achieve robust perfect adaptation under fluctuating conditions on a statistical average, local sensory systems exhibit nonadaptive fluctuations that are sensitive to the environmental ligand concentration. When the external chemoattractant concentration varies with both space and time, the chemotaxis motion becomes dampened at a rate controlled by the cell's adaptation rate (Jiang et al. 2010). These observations highlight the impact of noise on chemotactic behavior.

Chemotaxis model and response coefficient analysis

Soyer and Goldstein (2011) proposed recently a mathematical model for the chemotaxis of *E. coli* that extends earlier work and overcomes some of the weaknesses of previous models. Their model has five salient features which differentiate it from most other models: (i) finite bacterial tumbling times, (ii) finite rates of bacteria entering and exiting the tumbling state, (iii) three sub-populations of cells -- those traveling to the left, those traveling to the right and cells that are tumbling, (iv) a parameter that governs the sensitivity of the chemotaxis pathway, and (v) a Gaussian distribution of the chemoattractant that travels in the direction of fluid flow, i.e. to the right, in a microreactor tube. The *chemotactic performance* (CP) was measured in terms of the binding between the chemoattractant ligands and the corresponding chemoreceptors. Soyer and Goldstein's (2011) explanation for this choice, as opposed to the conventional choice of cellular movement *per se*, was that binding is the trigger that sets in motion a chain of events that ultimately generate cellular movement.

On this basis, Soyer and Goldstein (2011) proposed the equations of conservation given below for the three subpopulations of *E. coli* present in the microreactor.

$$\frac{dL}{dt} = (v + d) \frac{dL}{dx} - \alpha_L(x, t)L + \frac{\beta}{2}S \tag{1}$$

$$\frac{dR}{dt} = -(v - d) \frac{dR}{dx} - \alpha_R(x, t)R + \frac{\beta}{2}S \tag{2}$$

$$\frac{dS}{dt} = d \frac{dS}{dx} + \alpha_R(x, t)R + \alpha_L(x, t)L - \beta S \tag{3}$$

Equations (1)–(3) indicate that radial dispersion has been neglected; this may be a reasonable assumption in view of the small radius of a microtube and previous reports of radial dispersion being much smaller than axial dispersion (Rothstock et al. 2008, Sotowa et al. 2008). The rates at which the left-moving cells and the right-moving cells enter the tumbling state are characterized by α_L and α_R ; these parameters were considered to be modulated by a based rate α_0 , whereas β was assumed to be constant and equal for both types of cells. The second assumption implies that, after completing a tumble, a cell has equal probability of traversing left or right; this accounts for the presence of $\beta/2$ in Eqs.(1) and (2) and β in Eq.(3). To have a simple model with realistic features, Soyer and Goldstein

(2011) described the sensitivity of the chemotaxis pathway by a single lumped parameter λ . It may be clarified here that their notion of sensitivity departs somewhat from the conventional definition of sensitivity, which has been called the response coefficient here. They postulate that λ controls the level of modulation of α_0 by the chemotactic signal, which they refer to as the sensitivity.

While β is constant, α_L and α_R are described by the equations shown in Table 1. Soyer and Goldstein (2011) proposed a Gaussian distribution of the chemoattractant. This distribution was maintained in the present analysis for two reasons: (a) to be consistent with their work and (b) to be physically compatible with the residence time distribution in tubular flow with finite axial mixing (Danckwerts 1953, Gunther et al. 2004). In that case,

$$A(x) = \frac{e^{-x^2/2}}{\sqrt{2\pi}} \tag{4}$$

$$\text{and } A'(x) = \frac{dA}{dx} = -\frac{xe^{-x^2/2}}{\sqrt{2\pi}} \tag{5}$$

By equating $A'(x)$ and $A''(x)$ to zero, the corresponding maxima can be obtained as:

$$A_{\max} = \frac{1}{\sqrt{2\pi}} \quad (\text{at } x = 0) \tag{6}$$

$$A'_{\max} = \frac{e^{-1/2}}{\sqrt{2\pi}} \quad (\text{at } x = 1) \tag{7}$$

These expressions may be inserted in the equations for α_L and α_R in Table 1.

Now, the response coefficient, γ_{ij} , of any variable with respect to a parameter p_j may be defined as (Leaf et al. 1998):

$$\gamma_{ij} = \frac{\partial u_i}{\partial p_j} \tag{8}$$

Since the variables and the parameters may sometimes differ widely in their magnitudes and absolute variations, the γ_{ij} are usually normalized as:

$$\hat{\gamma}_{ij} = \frac{\gamma_{ij} p_j}{u_i} \tag{9}$$

Geevan et al. (1990) have shown that the response coefficients in a multi-variable multi-parameter system evolve with time according to:

$$\frac{d\hat{\gamma}_{ij}}{dt} = \sum_{k=1}^N J_{ik} \hat{\gamma}_{kj} + \frac{p_j}{u_i} \frac{\partial f_i}{\partial p_j}, \quad i = 1, \dots, M, j = 1, \dots, N \tag{10}$$

where M is the number of variables and N the number of parameters. From Soyer and Goldstein's (2011) model, it is clear that $N=4$, the parameters being α_0 , β , λ and d . To determine the value of M , we write Eqs.(1)–(3) in the general form:

$$\frac{\partial \bar{u}}{\partial t} = \bar{\phi}(\bar{u}, \bar{p}, \bar{u}') \tag{11}$$

where $\bar{u} = [L \ R \ S]^T$, $\bar{p} = [\alpha_0 \ \beta \ \lambda \ d]^T$ and \bar{u}' denotes the derivative of \bar{u} with respect to x . The superscript T denotes the transpose of a vector. Now we apply one-point orthogonal collocation (Villadsen and Stewart 1967) in x to reduce the three partial differential equations to six ordinary differential equations in time at the collocation points $x = \sqrt{1/3}$ and $x = 1$. Note that these are normalized distances. Equations (11) then become:

$$\frac{du_i}{dt} = f_i(\bar{u}, \bar{p}) \tag{12}$$

where $i = 1$ and 2 correspond to L at $x = \sqrt{1/3}$ and $x = 1$ respectively, $i = 3$ and 4 correspond similarly for R , and $i = 5$ and 6 for S . The equations for \hat{y}_{ij} , i.e. Eqs.(10), do not depend on x and hence do not have to be collocated. However, the collocated Eqs.(12) now indicate that $M = 6$. Therefore Eq.(10) contains $M \cdot N = 6 \cdot 4 = 24$ ordinary differential equations for the response coefficients; these were solved together with the six equations in Eq.(12).

For the initial conditions of Eq.(12) we recognize that at the start of chemotaxis there are equal numbers of cells moving to the left or right or tumbling. Therefore, considering that the total normalized concentrations of *E. coli* is unity, i.e. $L+R+S = 1$, we may apply the initial condition:

$$t = 0: L_i = R_i = S_i = 1/3; i = 1(1)6 \tag{13}$$

As explained by Geevan et al. (1990), the starting values of the response coefficients are zero; therefore:

$$t = 0: \hat{y}_{kj} = 0 \forall k, j \tag{14}$$

Now, Eqs.(10) and (12)–(14) define the complete problem comprising 30 ordinary differential equations with their initial conditions. These were solved numerically by the Runge-Kutta-Gill method with variable step size. Since our interest is in the response coefficients at the outlet of the microbio reactor, these coefficients for L_2 , R_2 and S_2 with respect to α_0 , β , λ and d are presented in Figures 2-13 and discussed in the next section. There are 12 sets of plots because Soyer and Goldstein (2011) applied their model to two types of responses of the cells: (a) linear and (b) adaptive. While the basic conservation equations remain the same, the equations for α_L and α_R differ between linear and adaptive responses (Table 1).

Table 1. Equations for the parameters α_L and α_R for *E. coli* cells with linear response and adaptive response (Soyer and Goldstein 2011).

Type of response	α_L	α_R
Linear	$\alpha_0 + \lambda \frac{A(x)}{A_{max}}$	$\alpha_0 + \lambda \frac{A(x)}{A_{max}}$
Adaptive	$\alpha_0 + \lambda \frac{(v+d)A(x)}{(v+d)A'_{max}}$	$\alpha_0 - \lambda \frac{(v-d)A(x)}{(v+d)A'_{max}}$

Application and Discussion

Soyer and Goldstein’s (2011) model [Eqs.(1)–(3)] has four basic parameters: α_0 , β , λ and d . Hence the response coefficients with respect to each of these parameters were computed according to Eqs.(10) and (12)–(14). The coefficients were determined for the two basic types of responses studied by them: (i) linear and (ii) adaptive. The values of the parameters differ between these two situations and so are the responses expected to be. These values are shown in Table 2.

Table 2. Values of the parameters used in the simulations (Soyer and Goldstein 2011).

Type of response	α_0	β	λ	d	v
Linear	0.01	0.02	3.6	0.01, 1.0	1.0
Adaptive	0.01	100.0	100.0	0.01, 1.0	1.0

Figures 2 to 13 portray the evolutions of the response coefficients with time for different situations. Apart from the cases described above, two rates of motion of the chemoattractant distribution

profile were also considered: (i) $d = 0.01$, which represents a distribution moving very slowly, i.e. nearly stationary, and (ii) $d = 1.0$, which characterizes a profile moving 100 times faster. By comparing d with v (Table 2), we also observe that for $d = 1.0$ the chemoattractant moves at a speed comparable to that of the bacteria. An overview of the 12 sets of response coefficients shown in the figures suggests that the responses of the population of cells differ widely in their nature as well as their magnitudes; thus it appears *prima facie* difficult to derive general inferences. However, a more detailed analysis reveals similarities and differences that follow certain patterns which provide insight into the behavior of the population of cells.

For the simplest case of linear bacterial responses in a slowly moving attractant pool, the response coefficient of bacteria moving to the left increase with time for β and d , and decrease for α_0 and λ . Bacteria moving to the right exhibit completely different responses: the former pair *decreases* as time advances, whereas the latter pair *increases*. There is, however, one similarity between the response coefficients with respect to β and d for the two bacterial populations. Both sets reach maxima (Figure 2) or minima (Figure 3) at the same time of about 14 min from the start. These observations are mutually compatible since the response of bacteria moving to the right and those moving leftward are qualitative mirror images of each other.

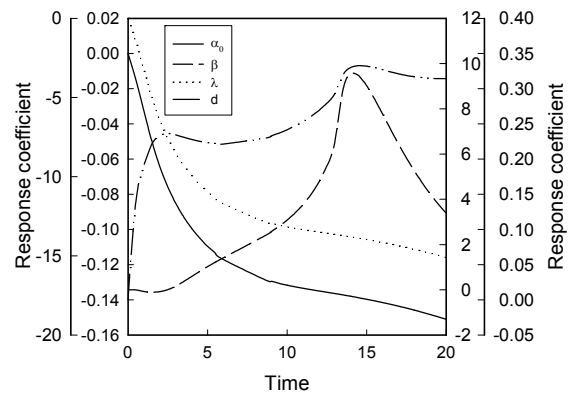


Figure 2. Response coefficient plots for left moving *E. coli* cells with linear response in a slow-moving chemoattractant concentration distribution.

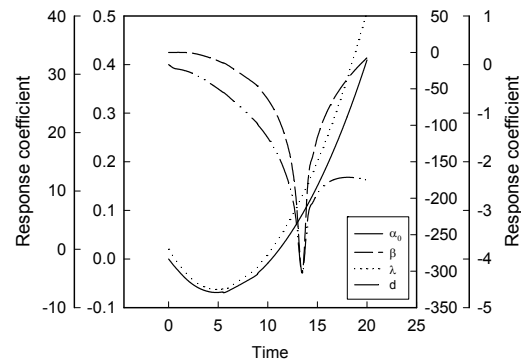


Figure 3. Response coefficient plots for right-moving *E. coli* cells with linear response in a slow-moving chemoattractant concentration distribution.

Bacteria that are in a state of tumbling have equal probability of moving left or right after the tumble is completed. Their response coefficients may therefore be expected to have some features of the left-moving and right-moving populations, and Figure 4 supports this inference. The equal probability of moving left or right for cells

currently in a tumbling state is also reflected in the peaks for α_0 and λ occurring at 7 min, which is one half the time at which the extrema are seen in Figures 2 and 3.

E. coli with adaptive responses display response coefficient profiles that are markedly different from those of cells with linear responses. However, self-consistency is preserved here too. Contrary to the profiles of Figures 2 and 3, the response coefficients in Figure 5 (for left-moving cells) and Figure 6 (for right-moving cells) are practically constant until about 14 min and then either decrease or increase sharply. However, there is a short interval (of about a minute) between these two phases during which the response coefficients pass through maxima (Figure 5) or minima (Figure 6). This transient phase could be a brief interlude of stochastic resonance, which will be discussed in further detail later.

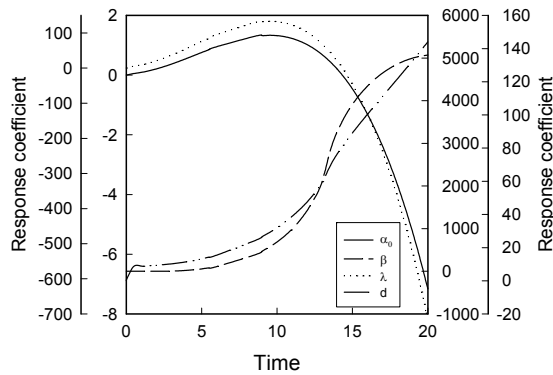


Figure 4. Response coefficient plots for tumbling *E. coli* cells with linear response in a slow-moving chemoattractant concentration distribution.

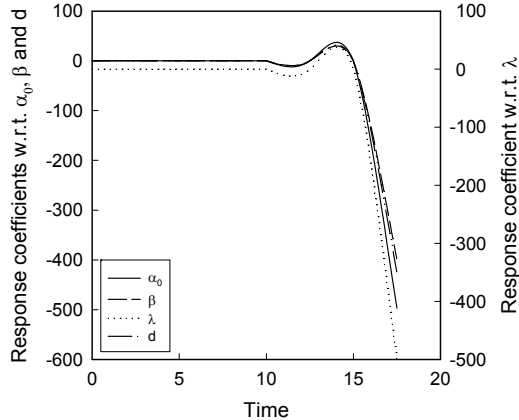


Figure 5. Response coefficient profiles for left-moving *E. coli* cells with adaptive response in a slow-moving chemoattractant concentration distribution.

Figure 7 has yet another feature that is in contrast with the corresponding profiles for linear response (Figure 4). Whereas for a linear response the cells in a state of tumbling have response coefficients that combine the features of the other two sub-populations, for an adaptive response the response coefficients are similar to those of cells moving to the left. This closeness to the behavior of one sub-population suggests that one effect of environmental noise is to bias the preference of the tumbling cells toward the left-moving population. The obvious question is: why should the bias be for this particular direction and not to the right? In the absence of conclusive experimental evidence, one conjecture is that since the environmental noise enters from the left through the

feed stream, and for a slow-moving distribution of the chemoattractant (recall that $d = 0.01$ in all cases) the fluctuations in the feed stream have sufficient time to influence the chemoreceptor-ligand binding kinetics, the cells in a tumbling state are more likely

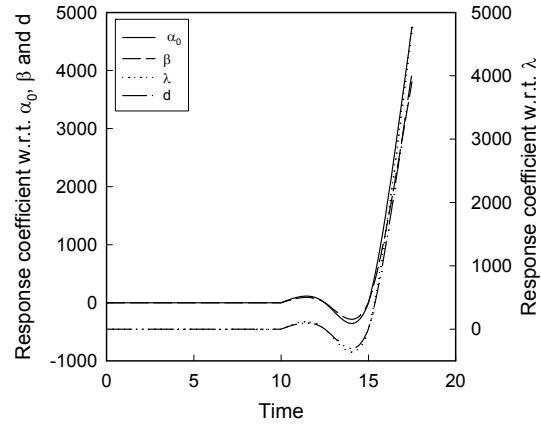


Figure 6. Response coefficient profiles for right-moving *E. coli* cells with adaptive response in a slow-moving chemoattractant concentration distribution.

to exhibit a behavior that is biased toward the source of the noise, i.e. toward the left. This might explain the similarity between the response coefficients of the tumbling cells and those of cells moving to the left.

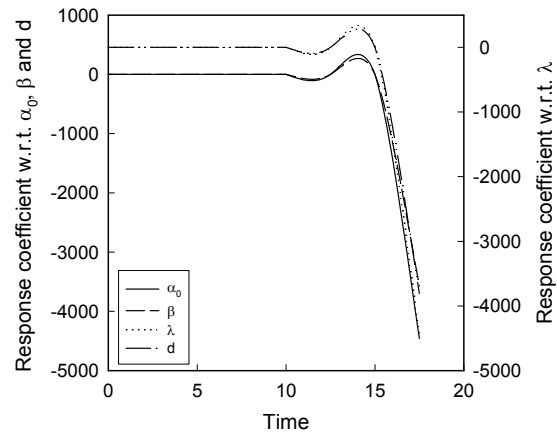


Figure 7. Response coefficient profiles for tumbling *E. coli* cells with adaptive response in a slow-moving chemoattractant concentration distribution.

For a chemoattractant concentration distribution that is moving fast toward the right ($d=1.0$), the response coefficients of the cells moving left-ward, i.e. away from the chemoattractant (Figure 8) are remarkably similar to those for adaptive response at $d=0.01$, (Figure 5). This anomalous ‘adaptive’ behavior may be explained by recognizing that when the bacteria and the chemoattractant move in opposite directions, and the latter is travelling fast, the cells ‘see’ little of the chemoattractant, except perhaps the tail portion of the Gaussian distribution of the attractant. The left-moving cells are thus ‘adapted’ to a region substantially depleted of the chemoattractant, so it is not surprising that bacteria with a normally linear response display (false) adaptive behavior. The falsity of this pseudo-adaptive behavior is also evident in the response coefficient

plot with respect to the rate of motion, d , of the chemoattractant in Figure 8. This plot is practically constant until about 4½ hours, after which it rises abruptly. During the constant phase, the cells moving

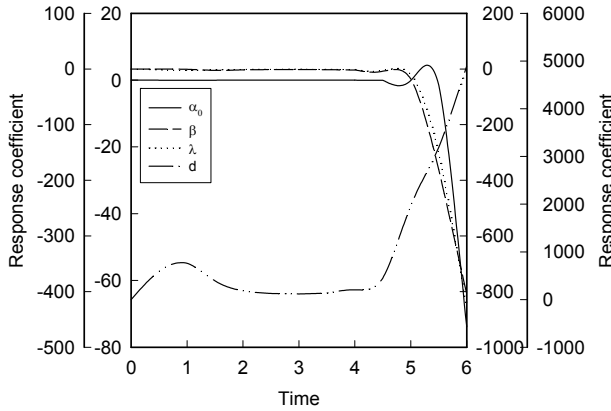


Figure 8. Response coefficient plots for *E. coli* cells with linear response moving to the left in a fast-moving chemoattractant concentration profile.

to the left are still within the wake of the Gaussian distribution, and the transition to the increasing regime signifies complete cut-off from the wake.

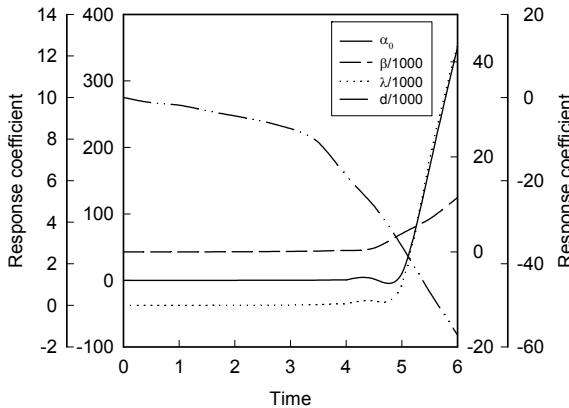


Figure 9. Response coefficient plots for *E. coli* cells with linear response moving to the right in a fast-moving chemoattractant concentration profile.

Despite the differences between the cases of a relatively static chemoattractant ($d=0.01$) and a concentration profile that is traveling much faster ($d=1.0$), internal consistency is maintained in both cases. As for $d=0.01$, the response coefficient plots for the bacteria moving to the right in a fast-moving chemoattractant field (Figure 9) are virtual mirror-images of those for the sub-population moving the other way (Figure 8) under the same conditions. This similarity is also maintained for the cells in a tumbling state, whose response coefficients (Figure 10) resemble those of the cells moving left (Figure 8) rather than those moving right. Hence the explanation offered for this observation in the case of $d=0.01$ is valid for $d=1.0$ also.

E. coli with adaptive responses display response coefficient profiles that are markedly different from those of cells with linear responses. However, self-consistency is preserved here too. Contrary to the profiles of Figures 2 and 3, the response coefficients in Figure 5 (for left-moving cells) and Figure 6 (for right-moving cells) are practically constant until about 14 min and then either decrease or

increase sharply. However, there is a short interval (of about a minute) between these two phases during which the response coefficients pass through maxima (Figure 5) or minima (Figure 6). This transient phase could be a brief interlude of stochastic resonance, which will be discussed in further detail later.

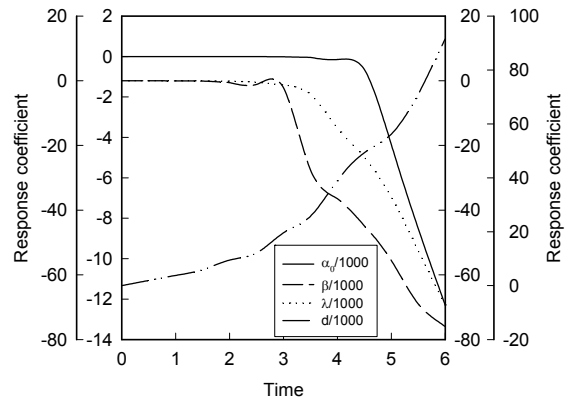


Figure 10. Response coefficient plots for tumbling *E. coli* cells with linear response in a fast-moving chemoattractant concentration profile.

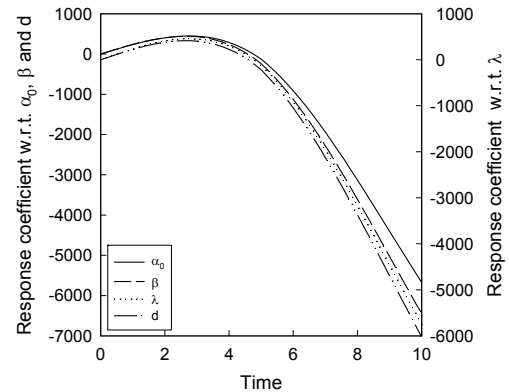


Figure 11. Response coefficient profiles for *E. coli* cells with adaptive response moving to the left in a fast-moving chemoattractant distribution.

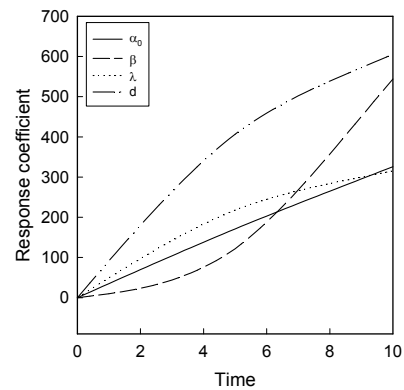


Figure 12. Response coefficient profiles for *E. coli* cells with adaptive response moving to the right in a fast-moving chemoattractant distribution.

The response coefficients of *E. coli* possessing an adaptive response (Figure 11-13) show trends that might seem unexpected. The coefficients either decrease or increase monotonically, barring a shallow maximum at around 4 h for cells moving to the left. This apparently anomalous behavior is discussed below. It may be noted,

however, that, regardless of the trends of the plots, the tumbling cells again have response coefficient profiles that are similar to those of the cells moving to the left, as observed also for adaptive responses with $d=0.01$ (Figure 7) and pseudo-adaptive responses with $d=1.0$ (Figure 10). Similar reasons therefore account for this resemblance, and the widely different situations in which it has been observed suggest that the phenomenon and its explanation may be universally true for *E. coli*.

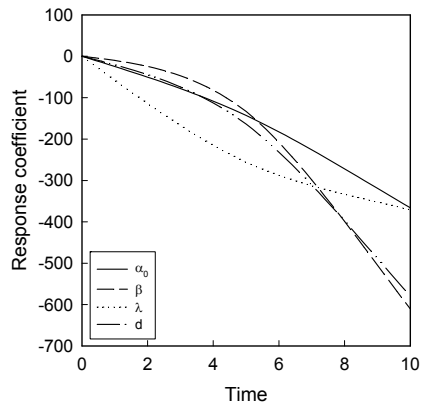


Figure 13. Response coefficient profiles for tumbling *E. coli* cells with adaptive response in a fast-moving chemoattractant concentration distribution.

An important semantic clarification is necessary for all the figures discussed. The terms ‘increasing’ or ‘decreasing’, or their synonyms, have been used to convey upward or downward trends. However, in terms of the magnitudes of the response coefficients, the absolute values of a ‘decreasing’ trend may actually be larger than those of an ‘increasing’ trend with which it is being compared. The magnitudes as well as the signs of the response coefficients are meaningful since they convey information about the nature of the responses to external noise. From this perspective, although the tumbling cells with a linear response in a slow-moving chemoattractant distribution (Figure 4) have some features of their left-moving (Figure 2) and right-moving (Figure 3) counter-parts, the magnitudes of the response coefficients are one to four orders of magnitude larger. For bacteria with adaptive responses under the same conditions, the tumbling cells have response coefficients (Figure 7) whose trends are similar to those of cells moving to the left (Figure 5) but magnitudes are closer to those of cells moving right (Figure 6). Nevertheless, the signs of the coefficients are again the same as those of the left-moving cells and opposite to that of the sub-population navigating to the right. Such partial similarities of the tumbling cells with the other two sub-populations are also seen for a fast-moving chemoattractant profile ($d=1.0$), and it occurs for both linear (Figure 8-10) and adaptive (Figure 11-13) responses.

In terms of magnitudes, it is also seen that, in general, (a) tumbling cells have much larger response coefficients than those moving to the left or right, and (b) the response coefficients for adaptive responses are larger than those for linear responses. The second observation might seem to contradict the ‘accepted’ conventional notion that adaptive behavior is a natural corollary of robust performance (Alon et al. 1999, Stelling et al. 2004). Clarifying this apparent contradiction, Patnaik (2007) explained that robustness merely implies that certain functional features are maintained in the presence of disturbances, but not all features. For instance, chemotactic motility may be robust but the adaptation time is not (Kollmann et al. 2005, Rao et al. 2004). Similarly, the present analysis is based on the chemotaxis model of Soyer and Goldstein (2011), who defined the chemotactic performance in terms of the

binding between the chemoreceptors and the chemical ligands; this process is external to the chemosensory network and is therefore not within the domain of the cell’s feed-back control mechanisms that contribute to robust perfect adaptation (Clausznitzer et al. 2010, Hamadeh et al. 2011, Hornung and Barkai 2008, Steuer et al. 2011). Moreover, as Nishikawa and Shibata (2010) have explained, even an adaptive chemosensory system may display nonadaptive fluctuations. This discussion also clarifies the observed ‘nonadaptive’ variations in the response coefficients for *E. coli* cells possessing adaptive responses in a rapidly moving chemoattractant concentration profile (Figures 11-13).

That nonadaptive dynamics is not an aberration is also explained by Goldstein and Soyer (2008), whose simulation studies showed that ‘stimulus scarcity and fluctuations result in complex pathway dynamics that result both in adaptive and nonadaptive dynamics’. These are precisely the conditions in which nonadaptive dynamics has been observed here. In their later work (Soyer and Goldstein 2011) they have drawn attention to the fact that previous observations that adaptive response dynamics provides optimal chemotactic performance (Celani and Vergassola 2010, Clausznitzer et al. 2010, Jiang et al. 2010, Patnaik 2007) had assumed tumbling to be instantaneous. However, although the duration of a tumble is about a tenth of the duration of a run (Berg 2000), it is not negligible, and accounting for the tumbling interval has indeed been shown to alter the optimal chemotactic performance (Celani and Vergassola 2010, de Gennes 2004, Goldstein and Soyer 2008).

It may be recalled that earlier in this discussion we had referred to short-duration maxima (Figures 2, 5 and 8) and minima (Figures 3, 6 and 9) observed in some situations. We may invoke the concept of stochastic resonance to explain these phenomena. However, we note first that the three maxima pertain to cells moving to the left, and the minima to cells travelling to the right under the same conditions. Thus, the concept of mirror images which was referred to earlier is maintained here also.

Stochastic resonance may be defined broadly as a ‘phenomenon where the presence of (controlled) noise in a nonlinear system is better for output signal quality than its absence’ (McDonnell and Abbott 2009). It is important to recognize in this definition that the system has to be nonlinear, which the chemotaxis framework of *E. coli* is. The word ‘controlled’ in parentheses has been inserted by this author because uncontrolled noise is often harmful whereas optimally controlled noise may be beneficial (Andrews et al. 2006, Chen et al. 2005, Patnaik 2012). Even though the control of environmental noise (through appropriate filters) was not implemented in this study, cells of *E. coli* and other bacteria have internal feedback systems that attenuate the propagation of noise (Andrews et al. 2006, Hamadeh et al. 2011, Hornung and Barkai 2008, Sartori and Tu 2011). The inflow of noise and the attenuation processes being complex, nonlinear and time varying, it is likely that during certain intervals of time the external noise inflow resonates with the intra-cellular noise systems and the results are observed as positive or negative increases in the response coefficients. Stochastic resonance has been postulated as a plausible explanation for enhanced performance not only in chemotaxis but a wide variety of biological processes (see McDonnell and Abbott (2009) and Hanggi (2002)] for examples).

Conclusions

Under natural conditions, bacteria such as *E. coli* experience noise within the cells and in the environment with which they interact. Different sources of noise vary differently with time and have both separate and combined effects on the functioning of the cells. One

significant effect is fluctuations in the values of the kinetic parameters of the reactions that govern the chemosensory network and its control of chemotaxis of the cells.

The role of uncertainty or variability in the kinetic parameters of the chemotaxis of *E. coli* in a microreactor was studied here through the response coefficients of the cells, derived from a chemotaxis model that considered three kinds of cells (a) those moving to the left at any instant of time, (b) those moving to the right, and (c) cells that are 'tumbling' and not 'running'. The time-dependent response coefficients of these three sub-populations of cells differed widely for two types of responses -- (a) linear and (b) adaptive -- and for two speeds of the chemoattractant concentration distribution -- (a) slow movement and (b) fast motion. The differences could, however, be reconciled both among the response coefficients themselves and with the cells' detection of a moving chemoattractant.

The results offered new insights into possible quantitative effects of environmental noise on the chemotaxis of *E. coli*. One noteworthy result was that although adaptive response confers robustness to bacterial chemotaxis for intra-cellular fluctuations, the influx of disturbances from outside may weaken robustness. Some features of the chemosensory system may even lose robustness through the impact of 'strong' disturbances, similar to that for intra-cellular and receptor-ligand binding noise. However, optimally filtered noise can improve chemotactic performance through stochastic resonance. This possibility is strengthened by performance enhancements observed for other biological systems through a similar process.

Nomenclature

All variables are dimensionless.

A	spatial concentration function of chemoattractant
A'	derivative of A with respect to x
A _{max}	maximum value of A
A' _{max}	maximum value of A'
d	rate of motion of the chemoattractant (to the right)
L	concentration of cells moving to the left
R	concentration of cells moving to the right
S	concentration of cells that are tumbling
t	time
v	swimming speed of the bacteria
x	distance along the microreactor length
α_0	parameter modulating basal values of α_L and α_R
α_L	rate at which left-moving cells enter the tumble state
α_R	rate at which right moving cells enter the tumble state
β	rate at which bacteria exit the tumble state
λ	parameter characterizing the sensitivity of the chemotaxis pathway
γ_{ij}	response coefficient of i-th variable with respect to j-th parameter
$\hat{\gamma}_{ij}$	normalized value of γ_{ij}

References

- Agyingi E, Maggelakis S, Ross D (2010) The effect of bacteria on epidermal wound healing. *Math Modeling Natural Phenom* 5: 28-39.
- Ahmed T, Shimizu TS, Stocker R (2010) Bacterial chemotaxis in linear and nonlinear steady microfluidic gradients. *Nano Lett* 10: 3379-3385.
- Alon U, Surette MG, Barkai N, Leibler S (1999) Robustness in bacterial chemotaxis. *Nature* 397: 168-171.
- Andrews BW, Yi Y-M, Iglesias PA (2006) Optimal noise filtering in the chemotactic response of *Escherichia coli*. *PLoS Comput Biol* 2: 1407-1418.
- Baker MD, Wolanin PW, Stock JB (2006) Systems biology of bacterial chemotaxis. *Curr Opin Microbiol* 9: 187-192.
- Berg HC (2000) Motile behavior of bacteria. *Phys Today* 23: 24-29.
- Briegleb A, Li X, Bilwes AM, Jensen GJ, Crane BR (2012) Bacterial chemoreceptor arrays are hexagonally packed trimers of receptor dimers networked by rings of kinase and coupling proteins. *Proc Natl Acad Sci USA* DOI:10.1073/pnas.1115719109.
- Celani A, Vergassola M (2010) Bacterial strategies for chemotaxis response. *Proc Natl Acad Sci USA* 107: 1391-1396.
- Chen L, Wang R, Zhou T, Aihara K (2005) Noise-induced cooperative behavior in a multi-cell system. *Bioinformatics* 21: 2722-2729.
- Clausznitzer D, Oleksink O, Lovdok L, Sourjik V, Endres RG (2010) Chemotactic response and adaptation dynamics in *Escherichia coli*. *PLoS Comput Biol* 6: e1000784.
- Danckwerts PV (1953) Continuous flow systems. Distribution of residence times. *Chem Eng Sci* 2: 1-13.
- de Gennes PG (2004) Chemotaxis: the role of internal delays. *Eur Biophys J* 33: 691-693.
- Francis NR, Wolanin PM, Stock JB, Derosier DJ, Thomas DR (2004) Three-dimensional structure and organization of a receptor/signaling complex. *Proc Natl Acad Sci USA* 101: 17480-17485.
- Geevan CP, Subba Rao J, Subba Rao G, Bajaj JS (1990) A mathematical model for insulin kinetics III: Sensitivity analysis of the model. *J Theor Biol* 147: 255-263.
- Goldstein RA, Soyer OS (2008) Evolution of taxis responses in virtual bacteria: Nonadaptive dynamics. *PLoS Comput Biol* 4: e100084.
- Gunther M, Schneider S, Wagner J, Gorges R, Henkel Th, Kielpinski M, Albert J, Bierbaum R, Kohler (2004) Characterization of residence time and residence distribution in chip reactors with modular arrangements by integrated optical detection. *Chem Eng J* 101: 373-378.
- Hamadeh A, Roberts MAJ, August E, McSharry PE, Maini PK, Armitage JP, Papachristodoulou A (2011) Feedback control architecture and the bacterial chemotaxis network. *PLoS Comput Biol* 7: e1001130.
- Hanggi P (2002) Stochastic resonance in biology. *ChemPhysChem* 3: 285-290.
- Hornung G, Barkai N (2008) Noise propagation and signaling sensitivity in biological networks: A role for positive feedback. *PLoS Comput Biol* 4: 0055-0061.
- Jiang L, Ouyang Q, Tu Y-H (2010) Quantitative modeling of *Escherichia coli* chemotactic motion in environments varying in space and time. *PLoS Comput Biol* 6: e1000735.
- Kaern M, Elston TC, Blake WC, Collins JJ (2005) Stochasticity in gene expression: From theories to phenotypes. *Nat Rev Genet* 6: 451-464.
- Kollmann M, Lovdok L, Bartholome K, Timmer J, Sourjik V (2005) Design principles of a bacterial signaling network. *Nature* 438: 504-507.
- Korobkova EA, Emonet T, Park H, Cluzel P (2006) Hidden stochastic nature of a single bacterial motor. *Phys Rev Lett* 96: 058105.
- Leaf TA, Srienc F (1998) Metabolic modeling of polyhydroxybutyrate biosynthesis. *Biotechnol Bioeng* 57: 557-570.
- McDonnell MD, Abbott D (2009) What is stochastic resonance? Definitions, misconceptions, debates and its relevance to biology. *PLoS Comput Biol* 5: e1000348.

- Nishikawa M, Shibata T (2010) Nonadaptive fluctuation in an adaptive sensory system: Bacterial chemoreceptor. *PLoS ONE* 516: e11224.
- Oleksink O, Jakovljeric V, Vladimirov N, Carvalho R, Paster E, Ryu WS, Meir Y, Wingreen NS, Kollmann M, Sourjik V (2011) Thermal robustness of signaling in bacterial chemotaxis. *Cell* 145: 312-321.
- Pandey G, Jain RK (2002) Bacterial chemotaxis toward environmental pollutants: Role in bioremediation. *Appl Environ Microbiol* 68: 5789-5795.
- Patnaik PR (2006) External, extrinsic and intrinsic noise in cellular systems: Analogies and implications for protein synthesis. *Biotechnol Mol Biol Rev* 1: 123-129.
- Patnaik PR (2007) Robustness analysis of the *E. coli* chemosensory system to perturbations in chemoattractant concentrations. *Bioinformatics* 23: 875-881.
- Patnaik PR (2008) Chemotaxis sensitivity of *Escherichia coli* to diffusion perturbations in narrow tubes. *The Open Chem Eng J* 2: 10-16.
- Patnaik PR (2012) Coupled filtering of environmental noise and ligand binding noise to improve the chemotaxis of *E. coli*. *IUP J Chem Eng* 4: 41-60.
- Paulsson J (2004) Summing up the noise in gene networks. *Nature* 427: 415-418.
- Paulsson J (2005) Models of stochastic gene expression. *Phys Life Rev* 2: 157-175.
- Paulsson J, Elf J (2006) Stochastic modeling of intra-cellular kinetics. In: *System Modeling in Cellular Biology*, MIT Press, Cambridge, MA, pp.149-174.
- Rao CV, Kirby JR, Arkin AP (2004) Design and diversity in bacterial chemotaxis: A comparative study in *Escherichia coli* and *Bacillus subtilis*. *PLoS Biol* 2: 0239-0252.
- Raser JM, O'Shea EK (2005) Noise in gene expression: Origin, consequences, and control. *Science* 309: 2010-2013.
- Rothstock S, Hessel V, Lob P, Werner B (2008) Characterization of a redispersion microreactor by studying its dispersion performance. *Chem Eng Technol* 31: 1124-1129.
- Samuel AD, Berg HC (1995) Fluctuation analysis of rotational speeds of the bacterial flagellar motor. *Proc Natl Acad Sci USA* 92: 3502-3506.
- Sartori P, Tu Y-H (2011) Noise filtering strategies in adaptive biochemical signaling networks: Application to *E. coli* chemotaxis. *J Stat Phys* 142: 1206-1217.
- Singh R, Olson MS (2008) Application of bacterial swimming and chemotaxis for enhanced bioremediation. In: Shah V (Ed) *Emerging Environmental Technologies*. Springer Science + Business Media, Berlin, Ch.7, pp. 149-172.
- Sourjik V, Berg HC (2002) Binding of the *Escherichia coli* response regulator CheY to its target measured *in vivo* by fluorescence resonance energy transfer. *Proc Natl Acad Sci USA* 99: 12669-12674.
- Sotowa K-I, Takagi K, Sugiyama S (2008) Fluid flow behavior and the rate of an enzyme reaction in deep microchannel reactor under high-throughput condition. *Chem Eng J* 135S: S30-S36.
- Soyer OS, Goldstein RA (2011) Evolution of response dynamics underlying bacterial chemotaxis. *BMC Evolution Biol* 11: 240.
- Stelling J, Sauer U, Szallasi Z, Doyle FJ, Doyle J (2004) Robustness of cellular functions. *Cell* 118: 675-685.
- Steuer R, Waldherr S, Sourjik V, Kollmann M (2011) Robust signal processing in living cells. *PLoS Comput Biol* 7: e1002218.
- Tindall MJ, Porter SL, Maini PK, Gaglia G, Armitage JP (2008a) Overview of mathematical approaches used to model bacterial chemotaxis I: the single cell. *Bull Math Biol* 70: 1525-1569.
- Tindall MJ, Maini PK, Porter SL, Armitage JP (2008b) Overview of mathematical approaches used to model bacterial chemotaxis II: bacterial populations. *Bull Math Biol* 70: 1570-1607.
- Tindall MJ, Gaffney EA, Maini PK, Armitage JP (2012) Theoretical insights into bacterial chemotaxis. *Syst Biol Med* 4: 247-259.
- Vaknin A, Berg HC (2004) Single-cell FRET imaging of phosphatase activity in *Escherichia coli* chemotaxis system. *Proc Natl Acad Sci USA* 101: 17072-17077.
- Villadsen JV, Stewart WE (1967) Solution of boundary value problems by orthogonal collocation. *Chem Eng Sci* 22: 1483-1501.
- Xu B-L, Tao Y (2006) External noise and feedback regulation: Steady state statistics of auto-regulatory genetic network. *J Theoret Biol* 6: 214-221.
- Yi T-Y, Iglesias P, Ingalls B (2000) Control theory in biology: From MCA to chemotaxis. <http://basi2.math.uwaterloo.ca/~bingalls/ICSB03tutorial/ICSB03InYilg.pdf>.